DOI: https://doi.org/10.17816/morph.634692

Bone tissue status in early stages of recovery after thermal exposure

Anna V. Gorokhova[1], Temur F. Nasibov[1], Ekaterina D. Porokhova[1, 2], Usman A. Bariev[1], Vladislav E. Nosov[1], Denis O. Pakhmurin[1, 2], Ilya I. Anisenya[2, 3], Pavel K. Sitnikov[2, 3], Igor A. Khlusov[1, 2]

[1] Siberian State Medical University, Tomsk, Russia;
[2] Tomsk State University of Control Systems and Radioelectronics, Tomsk, Russia;
[3] Tomsk National Research Medical Center, The Russian Academy of Sciences, Tomsk, Russia

ABSTRACT

BACKGROUND: Thermal ablation is a promising method for the treatment of bone tumors. However, to maximize the potential of this method, it is important to select the optimal dose/time ratio of high temperature exposure.

AIM: The aim of the study was to evaluate *in vivo* the response of rabbit bone tissue during early recovery (days 3 and 7) after local intraoperative hyperthermic ablation at 55–60°C in the medullary canal.

MATERIALS AND METHODS: The study used 6 outbred rabbits aged 15 weeks and weighing 3–4 kg. Animals were removed from the experiment on days 3 and 7 after local thermal ablation of the femoral diaphysis. Microscopic visual examination of bone tissue sections was performed after standard hematoxylin and eosin staining. In addition, the morphometric measurements were performed to determine area of non-mineralized bone matrix (Mallory staining); absorbance and area of osteoblast cytoplasm; absorbance and area of osteocyte nuclei (Einarson staining for nucleic acid detection). The results obtained were compared with those of the femur of the contralateral limb, which was not subjected to direct hyperthermia and served as a control. R-Studio, a free development environment for R programming language, was used to statistically process the data.

RESULTS: After high temperature exposure, histological sections of bone tissue stained with hematoxylin and eosin showed evidence of cellular abnormalities such as denucleated osteocytes and empty bone lacunae. Mallory staining showed no evidence of a negative effect of local thermal ablation on the intercellular bone matrix. Morphometry of Einarson stained sections showed an increase in osteoblast area on day 7 after exposure, with a decrease in their synthetic activity, signs of which were observed as early as day 3 of the experiment. There was also a decrease in the area and absorbance of osteocyte nuclei in the diaphysis of thermally ablated bones by day 3 after exposure. However, on day 7 after exposure, the area of nuclei in mature bone cells did not differ from the corresponding value in the contralateral limb. Considering the decrease in nuclei absorbance, the described changes may indicate colliquative necrosis of osteocytes.

CONCLUSIONS: Local intraoperative thermal ablation of the femoral diaphysis in rabbits at a marrow canal temperature of 55–60°C reduces the absorbance of osteoblast cytoplasm and osteocyte nuclei in the early recovery period, reflecting damage to the organelles of bone cells and disruption of metabolic processes in these cells. However, there was evidence of remodeling of the damaged area, presumably caused by migration of endosteal and periosteal cells from the metaphysis, which had not been exposed to direct hyperthermia. The results obtained may be useful for choosing the optimal regime (dose and duration) of high temperature exposure to bone tissue tumors, given the higher sensitivity of malignant cells to heating.

Keywords: rabbit; local thermal ablation; femur; histological sections; Einarson and Mallory staining; computer morphometry.

To cite this article:
Gorokhova AV, Nasibov TF, Porokhova ED, Bariev UA, Nosov VE, Pakhmurin DO, Anisenya II, Sitnikov PK, Khlusov IA. Bone tissue status in early stages of recovery after thermal exposure. *Morphology*. 2024;162(3):298–315. DOI: https://doi.org/10.17816/morph.634692

Submitted: 05.08.2024 **Accepted:** 01.11.2024 **Published online:** 04.12.2024

DOI: https://doi.org/10.17816/morph.634692

Состояние костной ткани в ранние сроки восстановления после термического воздействия

А.В. Горохова[1], Т.Ф. Насибов[1], Е.Д. Порохова[1, 2], У.А. Бариев[1], В.Е. Носов[1], Д.О. Пахмурин[1, 2], И.И. Анисеня[2, 3], П.К. Ситников[2, 3], И.А. Хлусов[1, 2]

[1] Сибирский государственный медицинский университет, Томск, Россия;
[2] Томский университет систем управления и радиоэлектроники, Томск, Россия;
[3] Томский национальный исследовательский медицинский центр РАН, Томск, Россия

АННОТАЦИЯ

Обоснование. Термоабляция — это перспективный метод лечения опухолей костной ткани. Однако для максимального раскрытия потенциала данного метода важен подбор оптимального соотношения дозы и времени высокотемпературного воздействия.

Цель — изучить *in vivo* реакцию костной ткани кроликов в ранний период восстановления (на 3 и 7 сутки) после локальной интраоперационной гипертермической абляции в диапазоне температур в костномозговом канале 55–60 °C.

Материалы и методы. Исследование проведено на 6 беспородных кроликах в возрасте 15 недель и массой 3–4 кг. Животных выводили из эксперимента на третьи и седьмые сутки после локальной термоабляции диафиза бедренной кости. Микроскопическое визуальное исследование срезов костной ткани проводили после стандартной окраски гематоксилином и эозином. Кроме того, морфометрически оценивали: площадь неминерализованного костного матрикса (окрашивание по методу Маллори); оптическую плотность и площадь цитоплазмы остеобластов; оптическую плотность и площадь ядер остеоцитов (окрашивание для выявления нуклеиновых кислот по методу Эйнарсона). Полученные результаты сравнивали со значениями для бедренной кости контрлатеральной конечности, не подвергавшейся прямой гипертермии и использованной в качестве контроля. Статистическую обработку данных выполняли с использованием свободной среды разработки R-Studio, предназначенной для языка программирования R.

Результаты. После высокотемпературного воздействия, на гистологических срезах костной ткани, окрашенных гематоксилином и эозином, отмечены признаки патологических изменений клеток — денуклеация остеоцитов и запустевание костных лакун. Окрашивание методом Маллори не выявило признаков негативного влияния локальной термоабляции на состояние межклеточного костного матрикса. Морфометрия срезов, окрашенных по Эйнарсону, показала увеличение площади остеобластов к седьмым суткам после воздействия на фоне снижения их синтетической активности, признаки которой были отмечены уже на третьи сутки эксперимента. К третьим суткам после воздействия также происходит уменьшение площади и оптической плотности ядер остеоцитов в диафизах костей, подвергшихся термоабляции. Однако, на седьмые сутки после воздействия площадь ядер в зрелых костных клетках не отличается от соответствующего значения в контрлатеральной конечности. На фоне снижения оптической плотности клеточных ядер описанные изменения могут свидетельствовать о развитии колликвационного некроза остеоцитов.

Заключение. Локальная интраоперационная термоабляция диафиза бедренной кости кроликов при температуре в костномозговом канале 55–60 °C снижает оптическую плотность цитоплазмы остеобластов и ядер остеоцитов в раннем восстановительном периоде, что отражает повреждение органелл костных клеток и нарушение метаболических процессов в них. Вместе с тем, обнаружены признаки ремоделирования повреждённого участка, предположительно обусловленные миграцией клеток эндоста и периоста из метафизов, которые не подвергались прямой гипертермии. Полученные результаты могут быть полезны для выбора оптимального режима (доза и продолжительность) высокотемпературного воздействия на опухоли костной ткани, при условии более высокой чувствительности злокачественных клеток к нагреванию.

Ключевые слова: кролики; локальная термоабляция; бедренная кость; гистологические срезы; окраска по Эйнарсону и Маллори; компьютерная морфометрия.

Как цитировать:
Горохова А.В., Насибов Т.Ф., Порохова Е.Д., Бариев У.А., Носов В.Е., Пахмурин Д.О., Анисеня И.И., Ситников П.К., Хлусов И.А. Состояние костной ткани в ранние сроки восстановления после термического воздействия // Морфология. 2024. Т. 162, № 3. С. 298–315. DOI: https://doi.org/10.17816/morph.634692

Рукопись получена: 05.08.2024 **Рукопись одобрена:** 01.11.2024 **Опубликована online:** 04.12.2024

DOI: https://doi.org/10.17816/morph.634692

热暴露后恢复早期骨组织的状况

Anna V. Gorokhova[1], Temur F. Nasibov[1], Ekaterina D. Porokhova[1, 2], Usman A. Bariev[1], Vladislav E. Nosov[1], Denis O. Pakhmurin[1, 2], Ilya I. Anisenya[2, 3], Pavel K. Sitnikov[2, 3], Igor A. Khlusov[1, 2]

[1] Siberian State Medical University, Tomsk, Russia;
[2] Tomsk State University of Control Systems and Radioelectronics, Tomsk, Russia;
[3] Tomsk National Research Medical Center, The Russian Academy of Sciences, Tomsk, Russia

摘要

论证。热消融是治疗骨肿瘤的一种有前景的方法。然而，为了最大限度地发挥该方法的潜力，选择高温暴露的剂量和时间的最佳比例非常重要。

目的 — 研究髓管内55～60℃温度范围内，局部高温消融术后恢复早期（第3天和第7天）兔骨组织的in vivo反应。

材料和方法。研究对象是6只年龄为15周，体重为3～4公斤的杂种兔。动物在股骨骨干局部热消融术后的第三天和第七天从实验中取出。用苏木精和伊红进行标准染色后，对骨组织切片进行显微目视检查。此外，还对以下各项进行形态测量评估：非矿化骨基质的面积（使用Mallory方法染色）；成骨细胞的光学密度和细胞质面积；骨细胞核的光学密度和面积（使用Einarson方法染色检测核酸）。将所得结果与未接受直接热疗的对侧肢体股骨的数值进行比较，并将其作为对照。使用专为R编程语言设计的R-Studio开发环境进行统计数据处理。

结果。高温暴露后，用苏木精和伊红染色的骨组织切片显示出细胞病理变化的迹象，即骨细胞去核和骨腔隙排空。Mallory方法染色未发现，局部热消融对细胞间骨基质状态产生负面影响的任何迹象。根据Einarson染色切片的形态测量显示，在暴露后第七天，成骨细胞的面积增加，而其合成活性却下降，这种迹象在实验的第三天就已显现。暴露后的第三天，经过热消融的骨干中骨细胞核的面积和光学密度也有所下降。但是在暴露后第七天，成熟骨细胞中的细胞核面积与对侧肢体中的相应值没有差异。在细胞核光学密度降低的背景下，所描述变化可能表明骨细胞发生液化性坏死。

结论。术中在骨髓管温度55～60℃下对家兔股骨骨干进行局部热消融，恢复早期成骨细胞细胞质和骨细胞核的光学密度降低，反映了成骨细胞细胞器的损伤及其代谢过程的破坏。与此同时，还发现了受损区域重塑的迹象，这可能是由于未接受直接热疗的干骺端中的骨内膜和骨膜细胞迁移所致。在恶性细胞对加热的敏感性较高的条件下，所获得的结果可能有助于选择骨组织肿瘤进行高温暴露的最佳模式（剂量和持续时间）。

关键词：兔子；局部热消融；股骨；组织学切片；Einarson和Mallory染色；计算机形态测量学。

To cite this article:
Gorokhova AV, Nasibov TF, Porokhova ED, Bariev UA, Nosov VE, Pakhmurin DO, Anisenya II, Sitnikov PK, Khlusov IA. 热暴露后恢复早期骨组织的状况. *Morphology*. 2024;162(3):298–315. DOI: https://doi.org/10.17816/morph.634692

收到：05.08.2024 **接受：**01.11.2024 **发布日期：**04.12.2024

BACKGROUND

The treatment of bone tumors, including osteosarcoma and metastatic invasion, remains one of the most challenging areas in oncology and is the focus of modern medical research. However, according to Menéndez et al. [1], the standards for bone tumor treatment have changed little since the late 1970s. Therefore, the search for innovative and promising therapeutic approaches for such tumors remains a pressing issue.

Thermoablation is considered a treatment of choice for both benign and malignant musculoskeletal tumors [2], provided that the anatomical integrity of the bone and its regenerative capacity are preserved. At the same time, factors involved in the regeneration of non-tumorous tissues, such as bone morphogenetic protein-2 (BMP-2), may enhance the proliferation of malignant cells in microscopic residual osteosarcoma nodules [3]. Therefore, it is of critical scientific and practical importance to identify best high-temperature exposure parameters (dose and duration) within the range of 55–100 °C, which can effectively eradicate tumor nodules while preserving the mechanical strength and regenerative potential of bone tissue. Previous studies have demonstrated that human bone tissue subjected *ex vivo* to hyperthermia in the 60–70 °C range retains its mechanical strength despite exhibiting moderate morphological signs of thermal damage [4].

AIM

To investigate the *in vivo* response of rabbit bone tissue in the early recovery period (on Days 3 and 7) following local intraoperative hyperthermic ablation at an intramedullary temperature of 55–60 °C.

MATERIALS AND METHODS

Study design

A single-center, prospective, controlled, randomized, open-label, experimental study was conducted.

Eligibility criteria

Inclusion criteria. The study used 6 outbred rabbits aged 15 weeks and weighing 3–4 kg. Prior to the experiment, the animals underwent a 7-day quarantine in ambient conditions.[1] After quarantine, the rabbits were randomly assigned to two study groups, with three rabbits in each group.

Non-inclusion criteria: signs of illness in animals, determined by a veterinary examination, including lethargy, loss of appetite, hair loss, skin and mucosal redness, itching, or ear mites.

Exclusion criteria: femoral fractures following thermoablation.

Study conditions

The study was conducted in the vivarium of the Central Research Laboratory of the Siberian State Medical University. The animals were housed individually in specialized labeled cages with bedding made of pre-sterilized dry wood shavings. The air temperature was maintained at 20–26 °C with a relative humidity of 40%–70%, under artificial lighting and forced ventilation. The rabbits were fed a standard, certified industrial feed (Biopro, DeltaFeeds, Russia) with a verified shelf life. Drinking water was available ad libitum.

Study duration

The study was conducted from August to November 2023. The assessment was performed during the early post-thermoablation period (Days 3 and 7), which is critical for subsequent reparative regeneration.

Description of medical intervention

Local intraoperative thermoablation of the right femur was performed *in vivo* using the Phoenix-2 local hyperthermia system (PromEl, Russia), developed at Tomsk State University of Control Systems and Radioelectronics [5]. The device is equipped with flexible heaters containing a resistive heating element that emits thermal energy when an electric current passes through it. Heat transfer to the target tissue occurs through conduction.

Premedication was carried out by intramuscular administration of 0.1% atropine (Moscow Endocrine Plant, Russia) at a dose of 0.5 mg/kg. General anesthesia was induced with an intravenous injection of a mixture of tiletamine and zolazepam (Zoletil 100, VIRBAC, France) at a dose of 0.2 mg/kg, 15 minutes after premedication. During surgery, additional doses of Zoletil 100 were administered as needed, ensuring that the total dose did not exceed the pre-calculated maximum allowable dose of 10 mg/kg per procedure.

Surgical procedures adhered to aseptic protocols. After triple antiseptic treatment of the surgical field with Miraxiderm Tris (MIRALEK, Russia), a longitudinal skin incision (up to 8 cm) was made. A sharp dissection was performed to expose the femur through the fibers of the biceps femoris muscle, followed by hemostasis. The femur was skeletonized using a raspatory. Outside the thermoablation zone, a perforation (2 mm in diameter) was made with a drill for the intramedullary insertion of a Pt 100 thermal sensor (PromEl, Russia) to monitor the temperature in the bone marrow cavity. A circular flexible surface heater and a thermal insulation material were applied to the exposed bone to confine the thermoablation impact to the designated area, preventing the involvement of surrounding tissues (Fig. 1).

Thermoablation (Fig. 1) was then performed following the established parameters (Table 1). Since the mean temperature in the medullary canal did not differ statistically

[1] Ambient conditions are standard, loosely controlled environmental conditions including temperature, lighting, humidity, ventilation, and noise.

between experimental groups during heating, a comparative dynamic assessment was feasible at 3 and 7 days post-surgery (Table 1).

Temperature readings in the medullary canal were recorded at one-minute intervals. The total exposure time was 20 minutes from the moment the lower threshold of the target temperature range was reached. The stabilization period to achieve an external (under the heater cuff) temperature of 60–65 °C was 3–5 minutes. After sensor insertion and upon completion of thermoablation, the skeletonized bone surface and surrounding soft tissues were rinsed with an antiseptic solution (Miraxiderm Tris, MIRALEK, Russia) and saline (Bionit, Russia). The surgical wound was then closed in layers with interrupted sutures using Vicryl 3/0 (Ethicon, Johnson & Johnson, USA): first the muscles, then the subcutaneous tissue, and finally the skin. A fine aluminum powder-based antiseptic (Aluminium Spray, Nicovet, Germany) was applied to the postoperative wound.

For five days post-surgery, all rabbits received intramuscular injections of: enrofloxacin (Doctor VIC, Belarus) at a dose of 5 mg/kg (antibiotic); meloxicam (Pharmstandard – UfaVITA, Russia) at a dose of 0.2 mg/kg (analgesic). The animals were euthanized using carbon dioxide asphyxiation: Group 1, 3 days after thermoablation; Group 2, 7 days after thermoablation.

Primary study outcome

A comparative analysis of morphofunctional damage characteristics in osteoblasts and osteocytes on histological sections of the rabbit femoral diaphysis on Days 3 and 7 after local intraoperative hyperthermic ablation.

Table 1. Experiment parameters

Group	Mean temperature, °C	Observation period after exposure, days
1 (*n*=3)	55,8±0,9	3
2 (*n*=3)	57,4±1,0	7

Note. The data are presented as the sample mean and sample standard deviation — M±SD; *n* — the number of animals in each group.

Group analysis

The study was conducted on crossbred rabbits of the same age, randomly assigned to two experimental groups. A comparative analysis of study outcomes was performed on Day 3 (n=3, Group 1) and Day 7 (n=3, Group 2) after local intraoperative hyperthermic ablation of the femur. The contralateral (intact) limb of each rabbit served as an intragroup control. Variational statistical methods were used for intergroup comparisons of independent sample indicators.

Methods of recording outcomes

Histological analysis of rabbit femurs was performed at the Department of Morphology and General Pathology of the Siberian State Medical University (Tomsk, Russia). Extracted intact and heat-exposed femurs were fixed in a 10% buffered aqueous formalin solution (pH 7.4, Biovitrum, Russia) for at

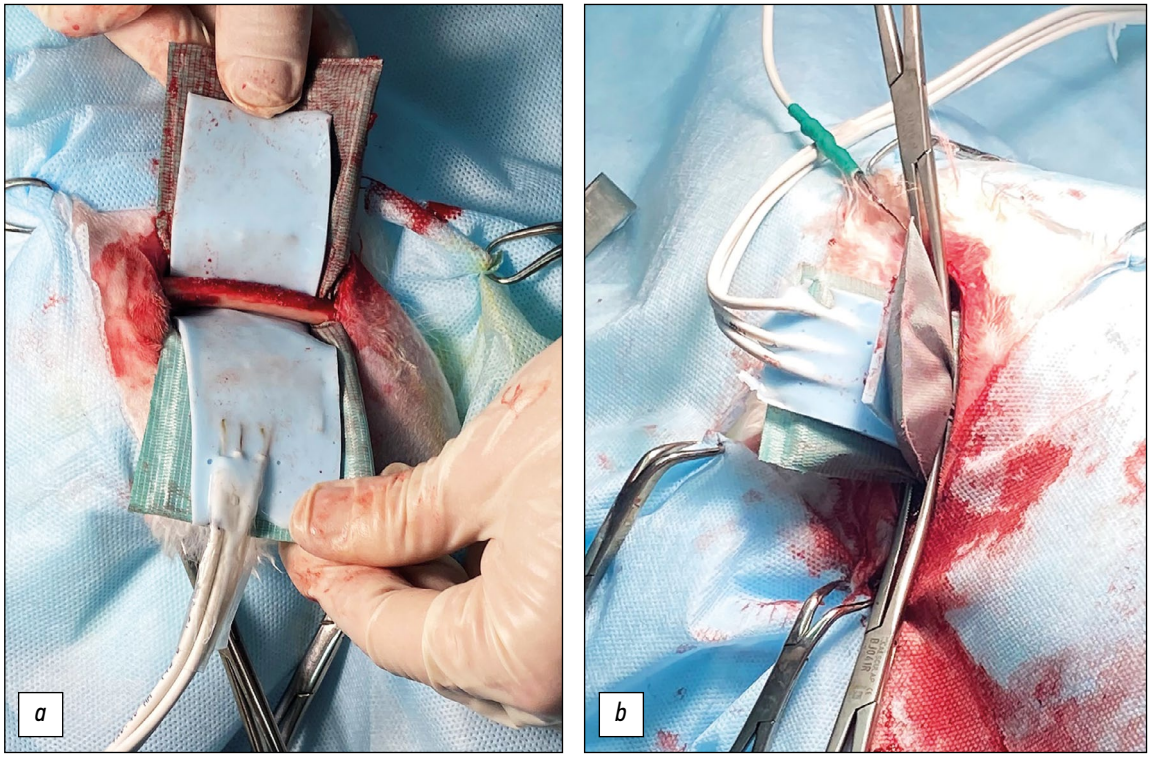

Fig. 1. Thermoablation: *a* — application of a heater and thermal insulating pad; *b* — bone heating.

least 24 hours at room temperature. Next, diaphyseal and proximal metaphyseal sections were isolated (Fig. 2), rinsed in tap water for 24 hours, and decalcified using a modified Grip's method. The decalcifying solution was a 1:1 mixture of 20% aqueous formic acid solution (Kupavnareaktiv, China) and 20% aqueous sodium acetate solution (Kupavnareaktiv, China), which was refreshed every two days for six days. The use of formic acid in the decalcifying mixture minimizes its impact on tissue staining properties [6]. The decalcified bone fragments were then placed in a 10% sodium sulfate solution (LenReaktiv, Russia) for 24 hours at room temperature, followed by a second 24-hour rinse in tap water at room temperature. The bone fragments were dehydrated through six isopropanol-based solution changes (IsoPrep, Biovitrum, Russia) following the manufacturer's protocol and embedded in HISTOMIX paraffin (Biovitrum, Russia). Bone paraffin sections (5–7 μm thick) were prepared using a semi-automatic microtome MZP 01 (Technom, Russia) and mounted on glass slides. The slides were stained with Gill's hematoxylin (Biovitrum, Russia) and eosin (Biovitrum, Russia) using a standard protocol. The effects of high-temperature exposure on bone structures were assessed by comparing them with tissues from the contralateral limb of the same rabbit.

The state of the intercellular bone matrix was evaluated on histological sections stained using the Mallory method(Labiko, Russia) in accordance with the manufacturer's recommendations. During staining, the collagen component of the non-mineralized bone matrix binds sequentially to phosphomolybdic acid and aniline blue, acquiring a dark blue color, whereas the mineralized bone matrix, which contains fewer collagen fibers, is stained red with fuchsin. Additionally, Einarson staining was performed as described in the literature [7]. Einarson's histochemical staining method allows for the assessment of osteoblast and osteocyte synthetic activity by visualizing nucleic acids within cells and evaluating their content in the nucleus and cytoplasm. This method is highly specific for nucleic acids, especially under acidic conditions [8]. In this study, all histological preparations were produced under identical conditions, ensuring that observed differences in morphofunctional characteristics reflect genuine tissue structural changes.

Histological preparations of the bones were examined using an Axioscope 40 light microscope (Zeiss, Germany). Digital photomicrographs were captured under standardized lighting conditions using a Canon PowerShot A2200 camera (14.1 MP, Canon Inc., China) and processed with AxioVision 4.8 software (Zeiss, Germany).

The area and optical density of stained regions of interest were assessed using computerized morphometry of digital images [9] with ImageJ software (version 1.38, National Institutes of Health, Bethesda, USA). Optical density measurements provided a quantitative characteristic of the opaque object using the formula:

$$D = 100 \times \log_{10} (S_F \div S_T)$$

where S_F is the background brightness; S_T is the brightness of the analyzed cell or tissue area in grayscale mode.

Ethical approval

The study design was approved by the IACUC Committee of the Central Research Laboratory of the Siberian State Medical University (Approval No. 1, April 3, 2023) and was deemed to comply with fundamental bioethical requirements.

Statistical analysis

Statistical analysis was conducted in RStudio (v. 2023.12.0 + 369) using the R programming language (version 4.4.0) and the following packages: MVN [10], stats [11], brunnermunzel [12]. Quantitative variables were tested for normality using the Shapiro-Wilk test with Royston's correction for large samples (Royston AS R94, 3⩽n⩽5000) [13].

Normally distributed quantitative variables are presented as the mean ± standard deviation (M ± SD); non-normally distributed quantitative variables are presented as the median and interquartile range (Me [Q1; Q3]).

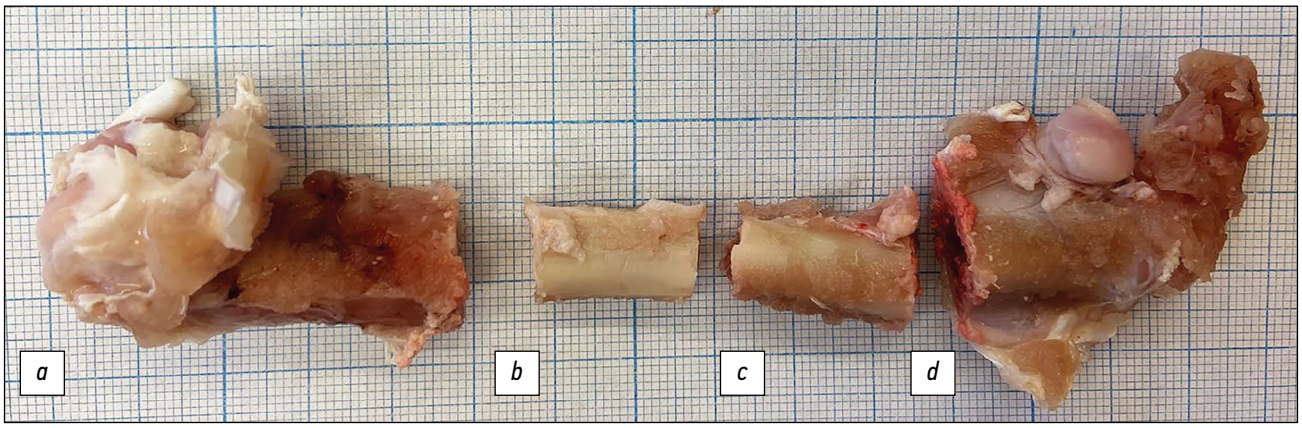

Fig. 2. Bone fragmentation scheme: *a* — distal epiphysis and metaphysis; *b* — diaphysis; *c* — proximal metaphysis; *d* — proximal epiphysis.

Mean values of normally distributed quantitative variables were compared using the Smith-Welch-Satterthwaite test [14–20]. For non-normally distributed quantitative variables, the Brunner-Munzel test was used [21–24].

RESULTS

Study objects

The study involved histological examination of thin sections of rabbit femoral bones (6 thermally ablated and 6 contralateral) divided into two groups (n = 3 per group) based on the duration of the recovery period. A total of 24 sections per rabbit were analyzed: 4 sections of each femur stained using three different methods—hematoxylin and eosin (H&E), Mallory's method, and Einarson's method. Morphometric measurements were performed on at least 30 individual cells (osteoblasts, osteocytes) or regions of interest.

Primary study results

In the control (contralateral, intact) femur, no signs of necrotic or inflammatory processes were observed in histological sections stained with hematoxylin and eosin at different recovery time points following intraoperative thermoablation. The compact bone tissue in the diaphysis was primarily composed of lamellar bone, and the bone marrow canal was filled with red bone marrow containing hematopoietic cells (Fig. 3*a*, *b*). The periosteum covered the outer bone surface and was connected to striated muscle fibers of typical structure (Fig. 3*c*). Numerous osteoblasts with morphological features of high synthetic activity were observed in periosteal cavities, characterized by a cylindrical cell shape, large volume, basophilic cytoplasm, and apically positioned nucleus (Fig. 3*d*).

Microscopic examination of H&E-stained sections revealed that localized hyperthermia (60–65°C under the heating cuff) did not cause significant distant damage to the contralateral femur within the observation period. This finding allows the morphometric parameters of the contralateral femurs to be used as control values (Table 2).

In the diaphyseal region of the thermally treated femurs, hematoma-like hemorrhages (Fig. 4*a*) and/or plasmastasis in the bone marrow canal near the endosteum (Fig. 4*c*) were observed. By Day 3, numerous empty osteocyte lacunae were present in the compact bone (Fig. 4*b*). By Day 7, in addition to empty osteocyte lacunae, destruction of the intercellular bone and cartilage matrix was observed in areas of perichondral osteogenesis (Fig. 4*d*). In both cases, these changes predominantly affected the periosteal region beneath the heating cuff. Since the flexible heating cuff was applied from the periosteal side, the observed empty lacunae suggest that periosteal temperatures were higher than those in the bone marrow canal.

In the proximal metaphysis, outside the direct heating zone, mechanical trauma was observed (Fig. 5*a*), attributed to temperature sensor insertion before heating. At the sensor insertion site (periosteal side), large amounts of cartilaginous and coarse-fibered bone tissue were formed (Fig. 5*b*). Numerous active osteoblasts and large osteoclasts were present in the periosteal and endosteal regions (Fig. 5*c, d*). Thus, by Day 7, active proliferation

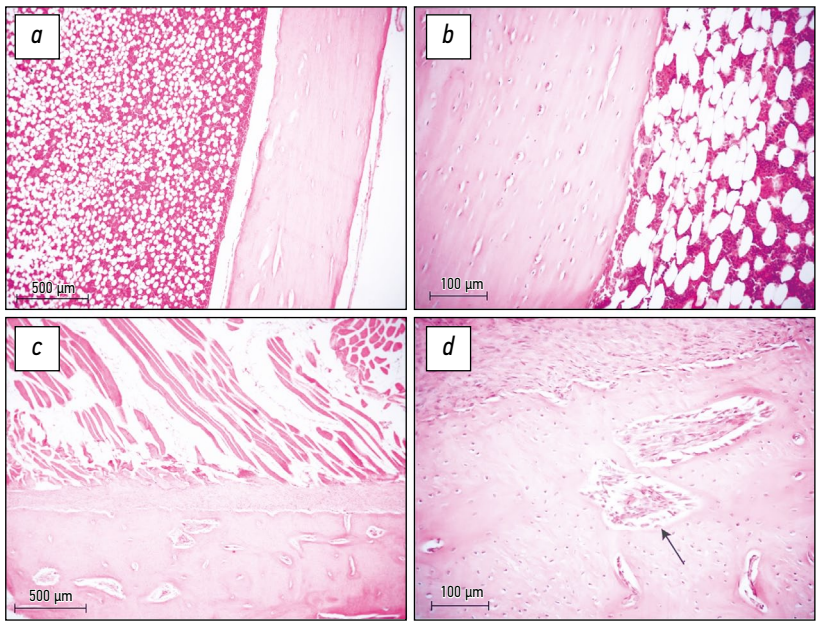

Fig 3. A section of an intact bone diaphysis: *a, b* — rabbit from group 1, lamellar bone tissue of the compact bone substance and red bone marrow in the medullary canal; *c, d* — rabbit from group 2, *c* — compact bone substance in the periosteal zone, striated muscle fibers of typical structure; *d* — numerous osteoblasts with morphological signs of high synthetic activity in the periosteal zone of bone (indicated by arrow). Hematoxylin and eosin staining, magnification: *a, c* — ×50; *b, d* — ×200.

Table 2. Morphometric indices of bone tissue state in contralateral control diaphysis of rabbits subjected to local thermoablation at an average medullary canal temperature of 55–60 °C

Parameter	Group 1 (Day 3) *n*=3	Group 2 (Day 7) *n*=3	Statistical significance level
Relative area of non-mineralized bone matrix	29,93±13,28 n_1=30	45,94±22,10 n_1=30	Welch's t-test, t=3.40; *p*=0.0014 *
Optical density of osteoblast cytoplasm, AU	5,80±1,68 # n_1=31	9,24±2,75 # n_1=38	Welch's t-test, t=6.38; *p* <0.001 *
Osteoblast cytoplasm area, μm^2	25,55[18,66; 30,07] n_1=31	18,72[15,04; 22,76] # n_1=38	Brunner-Munzel test, Brunner–Munzel Test Statistic = 2.31; *p*=0.025 *
Optical density of osteocyte nucleus, AU	13,45[11,83; 15,73] # n_1=60	10,25[8,72; 12,91] # n_1=60	Brunner-Munzel test, Brunner Munzel Test Statistic = 6.00; *p*=<0.001 *
Osteocyte nucleus area, μm^2	18,05[16,15; 23,04] # n_1=60	9,82[8,49; 11,97] n_1=60	Brunner-Munzel test, Brunner–Munzel Test Statistic = 16.94; *p* <0.001 *

Note. The data are presented as the sample mean and sample standard deviation — M±SD or as the median and the first and third quartiles — Me[Q1; Q3]; *n* — the number of animals in each group; y.e.o.n. (n.u.o.p.) — nominal units of optical density; n_1 — the number of examined areas or cells in each group; # — statistically significant differences with the diaphysis of the femurs subjected to thermal ablations, Brunner–Munzel criterion, *p* <0.05; * — statistically significant differences between groups 1 and 2.

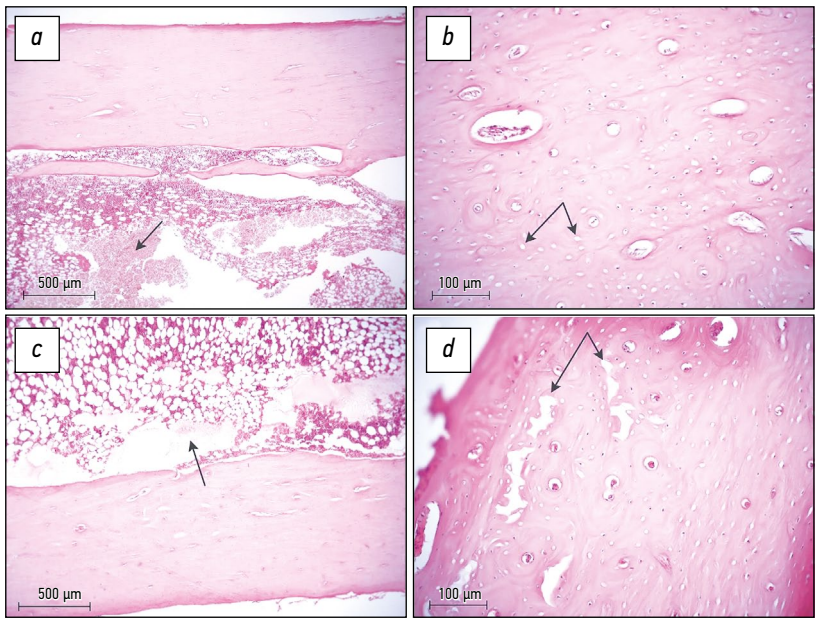

Fig. 4. A section of the femoral diaphysis after thermoablation at a temperature of 55–60°C in the medullary canal: *a, b* — rabbit from group 1 three days after heating; *a* — hematoma-type hemorrhages in the medullary canal (indicated by arrow); *b* — numerous deserted osteocyte lacunae in the periosteal zone of the bone (indicated by arrows); *c, d* — rabbit from group 2 seven days after heating; *c* — plasmostasis in the medullary canal near the endosteum (indicated by arrow); *d* — areas of destruction of intercellular bone and cartilage matrix in the periosteal zone of the bone (indicated by arrows). Hematoxylin and eosin staining, magnification: *a, c* — ×50; *b, d* — ×200.

of bone and cartilage cells in the metaphyseal region could contribute to diaphyseal regeneration via osteoblast migration.

Mallory staining revealed proliferation of coarse-fibered bone tissue in the periosteal zone of the proximal metaphysis (Fig. 5*e*). In the direct heating area (diaphysis), no visible evidence of severe thermoablation-induced damage to the intercellular bone matrix was detected compared to the contralateral limb. Osteoid fibers remained densely packed, and clear boundaries between bone lamellae in the compact bone were visible (Fig. 6). In Group 1 (Day 3) (Fig. 6*a*), mineralized matrix areas predominated compared to Group 2 (Day 7) (Fig. 6*b*), which was confirmed by computerized morphometry (Table 2).

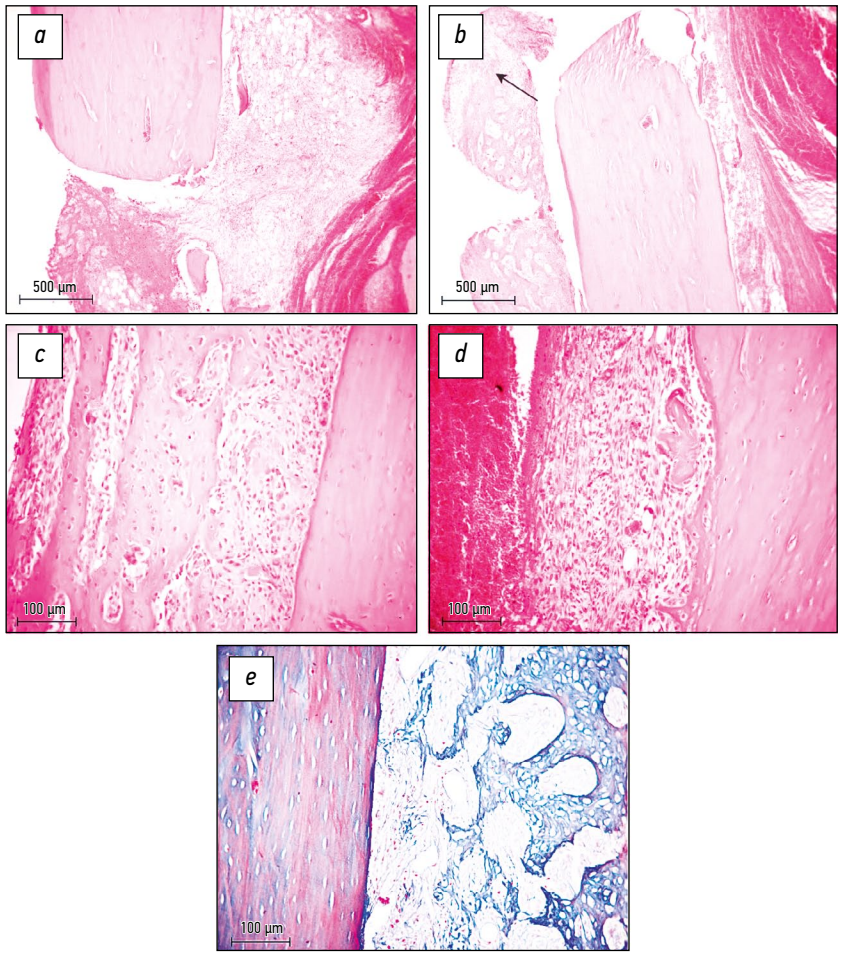

Fig. 5. A section through the proximal metaphysis of the rabbit femur seven days after heating the diaphysis to a temperature of 55–60 °C in the medullary canal: *a* — signs of mechanical trauma; *a, b, d* — hemorrhages; *b* — cartilage overgrowth (indicated by arrow); *e* — coarse fibrous bone overgrowth in the periosteal zone of the bone; *c* — numerous osteoblasts and large osteoclasts in the periosteal zone; *d* — numerous osteoblasts and large osteoclasts in the and endosteal zone of the bone. Staining: *a–d* — haematoxylin and eosin; *e* — Mallory's staining; magnification: *a, b* — ×50; *c, d, e* — ×200.

Einarson staining identified osteoblasts with high synthetic activity in the endosteal region. Large, polarized cells adhering to the bone surface with evenly distributed cytoplasmic RNA were evident, as indicated by intense staining (Fig. 7). Changes in relative optical density of osteoblast cytoplasm suggest altered synthetic activity and osteoid production capacity [25].

Since the study was conducted on non-inbred rabbits, statistically significant differences in collagen matrix structure and other morphometric characteristics were observed between groups (Table 2). Consequently, absolute values of parameters such as non-mineralized bone matrix area, osteoblast cytoplasm area, and optical density of osteoblast cytoplasm and osteocyte nuclei were not directly comparable. Therefore, a personalized statistical analysis approach was applied, standardizing values and comparing relative measurements. The dynamics of recovery after thermoablation are expressed as percentages relative to the intact femur (Table 3). The results indicate that in the direct heating zone (diaphysis), the proportion of non-mineralized bone matrix (Mallory staining) did not differ significantly from the contralateral femur at different recovery time points. Thus, at a thermoablation temperature of 60–65°C (with intramedullary temperature of 55–60°C), early regeneration-related changes in fibrous components are minimal due to the slow turnover rate of lamellar bone [25].

Morphometric assessment of osteoblasts in Einarson-stained sections (Fig. 7, Table 3) revealed a significant reduction in optical density and, consequently, synthetic activity in heated diaphyses. By Day 3, osteoblast cytoplasm optical density was 47.88% [41.94; 55.03] of the level in the intact bone. By Day 7, it further decreased to 39.31% [34.60; 51.33], which was significantly lower than on Day 3 (p=0.00028). However, osteoblast cytoplasm area (Table 3) remained unchanged by Day 3 (102.04% ± 28.89% relative to the intact diaphysis), but increased to 131% of the contralateral limb by Day 7 (p=0.0034), which was significantly higher than the Day 3 value (p=0.00052). This suggests that by Day 7, there was a higher proportion of larger, younger osteoblasts, likely due to migration from the metaphyseal defect caused by temperature sensor insertion.

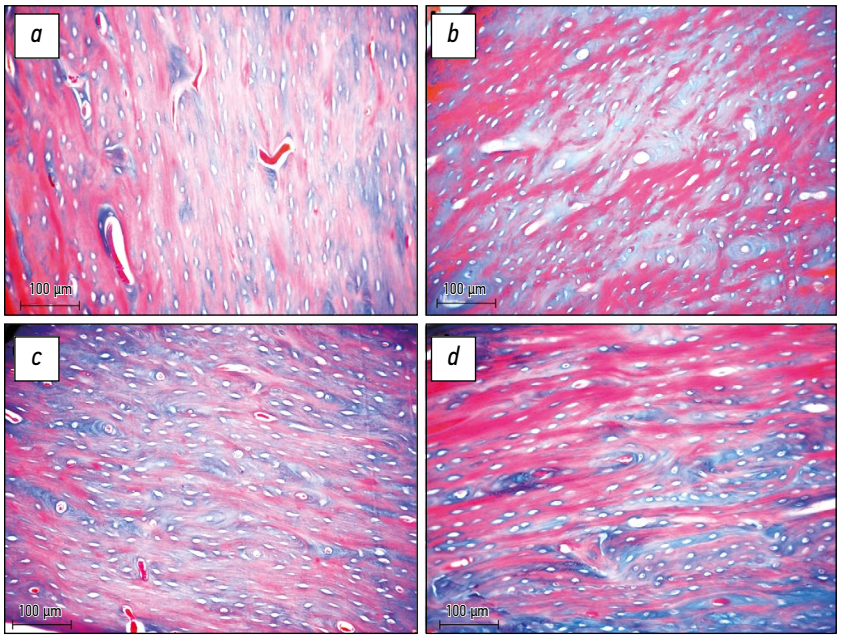

Fig. 6. A section through the diaphysis of femur: *a, c* — intact bone; *a* — rabbit from group 1; *c* — rabbit from group 2; *b, d* — diaphysis of rabbit bone after heating at a temperature of 55–60 °C in the medullary canal; *b* — rabbit from group 1 three days after heating; *d* — rabbit from group 2 seven days after heating; *a–d* — bone plates of compact bone substance with clear boundaries, fibrous components of osteoid tightly adhering to each other. Mallory staining, magnification ×200.

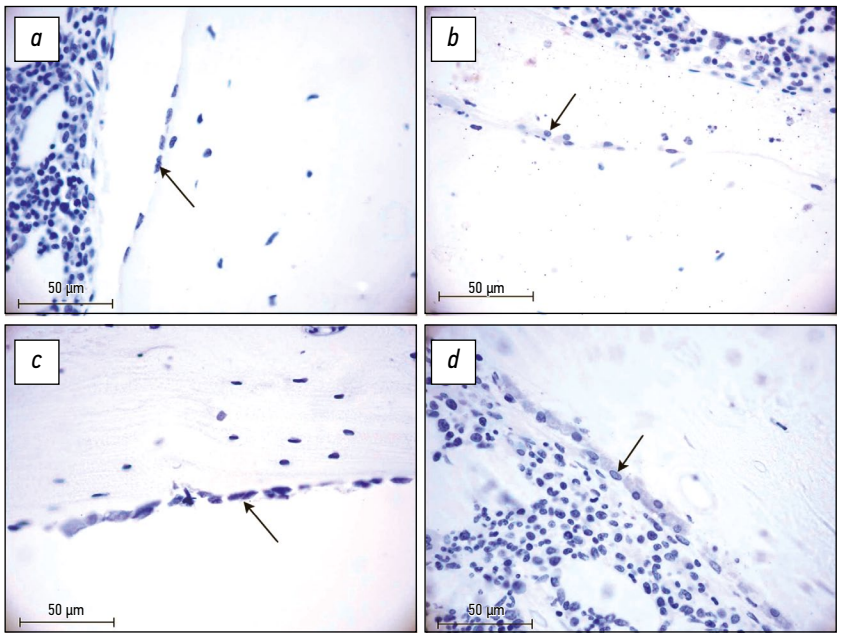

Fig. 7. A section through the femoral diaphysis in the endosteal zone: *a* — intact bone of rabbit from group 1; *c* — intact bone of rabbit from group 2; *b* — femur of group 1 three days after heating; *d* — femur of rabbit from group 2 seven days after heating at a temperature in the medullary canal of 55–60 °C.; *a, c* — osteoblasts with morphological signs of high synthetic activity (indicated by arrows); *b, d* — osteoblasts with morphological signs of low synthetic activity (indicated by arrows). Einarson staining, magnification ×630.

During staining histological sections of rabbit femurs using the Einarson method, information was obtained regarding the presence of DNA molecules in osteocyte nuclei and, to a lesser extent, RNA. Since osteocytes are a conserved cell population with low synthetic activity, nucleic acids were predominantly visualized in nuclei, while cytoplasm remained unstained (Fig. 8*a, c*). In the diaphysis of the femur of the intact limb in Group 1 rabbits, the compact bone is predominantly composed of parallel-arranged bone lamellae. Lacunae containing osteocytes with large, round nuclei, which stain intensely using the Einarson method, are visible between the lamellae (Fig. 8*a*). In the compact bone of the intact femur in Group 2, osteocytes with elongated, spindle-shaped nuclei are more frequently observed (Fig. 8*c*). In the compact bone of heat-exposed femurs (Fig. 8*b, d*), on Days 3 and 7, empty osteocyte lacunae or osteocytes with elongated,

Table 3. Comparison of morphometric indices of rabbit femoral diaphysis at different times after local thermoablation at an average medullary canal temperature 55–60 °C, in % of values for the contralateral diaphysis

Parameter	Group 1 (Day 3) *n*=3	Group 2 (Day 7) *n*=3	Statistical significance level
Relative area of non-mineralized bone matrix, %	109,59±42,47 n_1=30	114,14±40,93 n_1=30	Welch's t-test, t=0.42; *p*=0.67
Optical density of osteoblast cytoplasm, %	47,88[41,94; 55,03] # n_1=35	39,31[34,60; 51,33] # n_1=32	Brunner-Munzel test, Brunner–Munzel Test Statistic=2.76; *p*=0.00028 *
Osteoblast cytoplasm area, %	102,04±28,89 n_1=35	130,94±34,95 # n_1=32	Welch's t-test, t=3,67; *p*=0,00052 *
Optical density of osteocyte nucleus, %	94,76±14,69 # n_1=60	90,00±30,79 # n_1=60	Welch's t-test, t=-1,08; *p*=0,28
Osteocyte nucleus area, %	46,84[42,29; 53,29] # n_1=60	108,16[71,56; 152,83] n_1=60	Brunner-Munzel test, Brunner–Munzel Test Statistic =-15,43; *p* <0,001 *

Note. The data are presented as the sample mean and sample standard deviation — M±SD or as the median and the first and third quartiles — Me[Q1; Q3]; *n* — the number of animals in each group; n_1 — the number of examined areas or cells in each group; # — statistically significant differences with the corresponding control (intact diaphyses, Table 2, Brunner–Munzel criteria, *p* <0.05); * — statistically significant differences between groups 1 and 2.

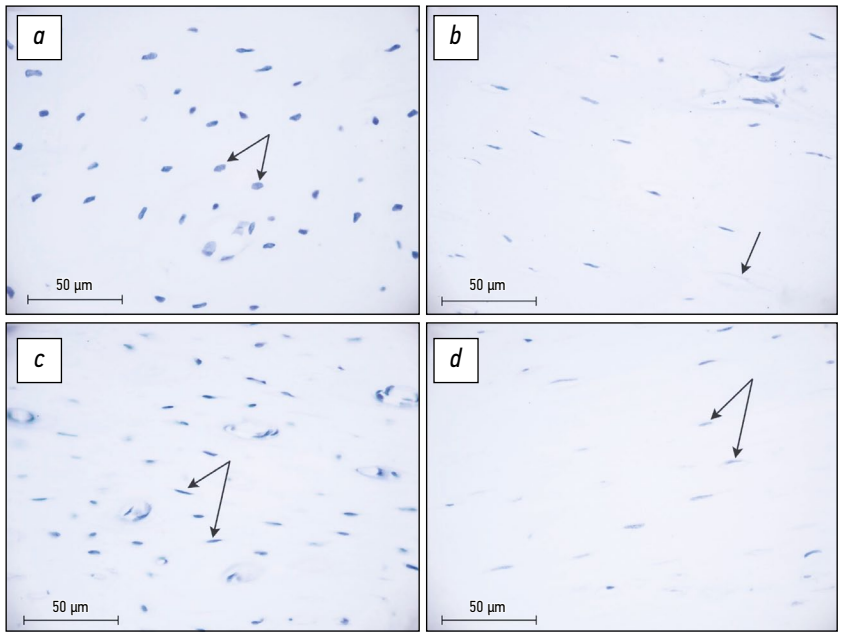

Fig. 8. A section through the compact substance of the femoral diaphysis: *a* — intact bone of rabbit from group 1, osteocytes with large, round, intensely stained nuclei (indicated by arrows); *c* — intact bone of rabbit from group 2, osteocytes with fusiform, intensely stained nuclei (indicated by arrows); *b* — femoral diaphysis of rabbit from group 1 three days after heating at a temperature in the medullary canal of 55–60 °C, deserted osteocyte lacunae (indicated by arrow); *d* — femoral diaphysis of rabbit from group 2 seven days after heating, osteocytes with less intensely stained fusiform nuclei (indicated by arrows). Osteocyte staining by the Einarson method, magnification ×630.

spindle-shaped nuclei with a visibly smaller staining area and lower optical density of the nuclei, compared to the corresponding intact diaphysis (Fig. 8*a, c*), were observed.

Computerized morphometry (Table 3) demonstrated a similar reduction (p=0.28) in osteocyte optical density in heated diaphyses across both groups. However, optical density in heated femurs was significantly lower than in contralateral diaphyses (Brunner-Munzel test, p<0.05). By Day 3 after hyperthermic exposure, the osteocyte area sharply decreases to 46.84% [42.29; 53.29] of the level in the contralateral bone. However, by Day 7, their size nearly returns to baseline values, reaching 108% of the measurement in the contralateral femur. This suggests rapid osteocyte population renewal, likely driven by larger, younger cells with low synthetic activity, similar to osteoblasts.

DISCUSSION

Summary of the primary study results

Histological sections of rabbit femoral diaphyses stained with hematoxylin and eosin after high-temperature exposure showed signs of pathological cellular changes, including osteocyte denucleation and empty bone lacunae. Morphometric analysis of Einarson-stained sections revealed an increase in osteoblast area by Day 7, despite a decline in their synthetic activity, which was already evident by Day 3. By Day 3, osteocyte nuclei area and optical density decreased in thermally ablated femoral diaphyses. However, by Day 7, the osteocyte nuclei area in mature bone cells returned to values comparable to the contralateral limb. The reduction in nuclear area alongside decreased optical density suggests the development of colliquative necrosis of osteocytes.

Discussion of the primary study results

The early postoperative period, spanning several days post-surgery, is crucial for bone healing during osteosynthesis and endoprosthetic procedures [26]. Therefore, the present study focused on early-stage post-surgical bone regeneration following localized thermoablation in non-inbred rabbits, an animal model widely used in bone and joint tissue research [27].

Our study revealed significant variability in morphometric parameters of femoral bones not directly subjected to thermoablation, which mirrors interindividual variations in human bone tissue [28]. However, the contralateral femoral diaphysis of rabbits undergoing localized thermoablation should be considered only conditionally intact. In Group 2 (Day 7 post-hyperthermia), higher regeneration markers (e.g., osteoblast cytoplasm optical density and area) were observed compared to Group 1 (Day 3), whereas osteocyte morphometric parameters declined (Table 2). Based on these findings, we propose a hypothesis of distant thermoablation effects on bone tissue, potentially mediated by bioactive substances released during direct hyperthermia of the opposite femoral diaphysis. Transforming growth factor-beta (TGF-β) and insulin-like growth factor 1 (IGF-1) are known to be released from the bone matrix during resorption and stimulate osteoblastic differentiation of mesenchymal stem cells [29–31]. Pro-inflammatory cytokines (e.g., IL-1, IL-6) secreted into circulation during extreme conditions [32] can also induce bone regeneration, particularly in hematoma formation scenarios [33].

Given this context, statistical processing and comparisons were conducted following the principles of personalized biomedicine. For each animal, morphometric indices were normalized to contralateral values, which served as internal controls (Table 3).

According to Einarson's highly specific nucleic acid staining method [8], by Day 7 post-direct thermoablation, osteoblast cytoplasmic area increased by 30% compared to the control, along with osteocyte area expansion. We hypothesize that rapid osteoblast population turnover in heated diaphyses is facilitated by migration of young cells from unaffected femoral regions.

By Day 7, pronounced reparative regeneration and hyperplasia of cartilaginous and coarse-fibered bone tissue were observed in the mechanical defect zone in the metaphysis, particularly from the periosteal side (Fig. 5). This is likely linked to hematoma formation, both in the diaphysis (Fig. 4*a*) and in the metaphyseal defect zone created by temperature sensor insertion (Fig. 5*a, b, d*). Hematomas are essential for bone regeneration [34], as they exhibit osteogenic [35] and angiogenic properties [36], mediated by their cellular composition and biologically active molecules essential for tissue healing [37].

Early reparative regeneration in the non-heated metaphyseal region may serve as a source of migrating mesenchymal stromal stem cells and (pre)osteoblasts, which travel along the endocortical surface toward lamellar bone diaphysis restoration. However, osteoblast synthetic activity remained reduced in both the 3-day and 7-day recovery periods following localized intraoperative hyperthermic ablation at 55–60°C in the medullary canal. This may be attributed to persistent thermal damage to bone cells and a predominance of cellular migration over differentiation, ensuring rapid restoration of bone mass similar to hematopoietic system regeneration.

The significant changes in nucleic acid content, primarily RNA, in osteoblast cytoplasm post-direct thermal exposure suggest that nucleic acids may serve as primary targets of high-temperature-induced cellular shock. Thermal shock is known to disrupt RNA synthesis, processing, and transport [38]. *In vitro* studies have shown that brief (10 min) hyperthermia at 42 °C causes denaturation and condensation of ribosomal RNA, leading to polysome disassembly into single organelles [39]. Additionally, hyperthermia disrupts mRNA structure [40].

Study limitations

The significant morphometric variability in rabbit femoral diaphyses not subjected to direct thermoablation necessitated

reporting results in relative (percentage) units. Differences in contralateral control bone tissue status may stem from: variability in physiological bone regeneration rates among non-inbred rabbits; distant systemic effects of intraoperative thermoablation on the opposite limb in the early post-hyperthermic period. Nevertheless, the comparative findings of this study are highly valuable, as they describe the localized effects of thermoablation while accounting for its potential systemic influence through integral regulatory mechanisms.

CONCLUSION

Thermoablation is considered a promising method for the treatment of bone tumors, provided that the anatomical integrity of the bone and its regenerative capacity are preserved. *Ex vivo* studies have demonstrated moderate thermal damage to human bone tissue while maintaining its mechanical strength after hyperthermia at 60–70 °C [4]. Therefore, investigating the *in vivo* response of rabbit bone tissue following local intraoperative hyperthermic ablation in the 55–60 °C range in the medullary canal has significant scientific and practical interest.

The early postoperative period (within a few days after surgery) is considered critical for bone healing following osteosynthesis and endoprosthetic procedures [26]. The dynamic *in vivo* study of rabbit bone tissue in the early recovery phase (Day 3 and Day 7) after local intraoperative thermoablation of the femoral diaphysis revealed no changes in the percentage ratio of non-mineralized to mineralized matrix in lamellar bone, regardless of the recovery period. This may be due to the mild damaging effect of the selected temperature range on the fibrous component of bone tissue, the slow turnover rate of lamellar bone and/or the low sensitivity of the staining method used.

However, by Day 7 post-hyperthermia, hematoxylin and eosin staining revealed empty osteocyte lacunae and denucleation of mature bone cells, which are morphological markers of cell death through apoptosis and/or necrosis. Significant changes in bone cells were also detected using Einarson's nucleic acid staining. In the thermoablated diaphyseal zone, there was a marked decrease in the optical density of osteoblast cytoplasm (by 50%–60%) and osteocytes (by 5%–10%), indicating the damaging effects of thermoablation at 55–60 °C on cellular metabolism and intracellular organelles of healthy bone cells, primarily the nucleus and ribosomes, which regulate synthetic activity.

At the same time, the appearance of enchondral osteogenesis sites in the periosteal zone indicates the initiation of remodeling in the thermoablated area. Among other factors, such remodeling may be associated with reparative regeneration induced by mechanical trauma in the metaphyseal region following the insertion of the thermal sensor. Tumor cell nucleic acids are also highly sensitive to heat [38]. Therefore, the preservation of bone regenerative capacity at a 55–60 °C exposure, coupled with the death and suppression of synthetic activity in both healthy and tumor cells, may provide an effective strategy for tumor eradication, given the higher thermal sensitivity of malignant cells within this temperature range.

ADDITIONAL INFORMATION

Funding source. This work was financially supported by the Ministry of Science and Higher Education of the Russian Federation, project number FEWM-2024-0003.

Competing interests. The authors declare that they have no competing interests.

Authors' contribution. All authors made a substantial contribution to the conception of the work, acquisition, analysis, interpretation of data for the work, drafting and revising the work, final approval of the version to be published and agree to be accountable for all aspects of the work. A.V. Gorokhova — experimental procedures, collection and analysis of literature sources, writing and editing the article; T.F. Nasibov — histological study, statistical analysis of data; E.D. Porokhova — experimental procedures, histological study; U.A. Bariev — histological study and morphometric analysis of data; V.E. Nosov — experimental procedures; D.O. Pakhmurin — experimental procedures; I.I. Anisenya — experimental procedures; P.K. Sitnikov — experimental procedures; I.A. Khlusov — collection and analysis of literary sources, writing and editing the article.

REFERENCES

1. Menéndez ST, Gallego B, Murillo D, et al. Cancer Stem Cells as a Source of Drug Resistance in Bone Sarcomas. *J Clin Med*. 2021;10(12):2621. doi: 10.3390/jcm10122621

2. Ringe K, Panzica M, von Falck C. Thermoablation of Bone Tumors. *Rofo*. 2016;188(6):539–550. doi: 10.1055/s-0042-100477

3. Kendal JK, Singla A, Affan A, et al. Is Use of BMP-2 Associated with Tumor Growth and Osteoblastic Differentiation in Murine Models of Osteosarcoma? *Clin Orthop Relat Res*. 2020;478(12):2921–2933. doi: 10.1097/corr.0000000000001422

4. Pakhmurin D, Pakhmurina V, Kashin A, et al. Mechanical and Histological Characteristics of Human Tubular Bones after Hyperthermal Treatment. *Symmetry*. 2023;15(1):156. doi: 10.3390/sym15010156

5. Pakhmurin DO, Pakhmurina VV, Anisenya II, Sitnikov PK. Experimental study of the temperature distribution in long tubular bones with a periossal arrangement of heaters. *Siberian Journal of Oncology*. 2023;22(2):65–75. EDN: TLRZUE (In Russ.) doi: 10.21294/1814-4861-2023-22-2-65-75

6. Sarkisov DS, Perov YL, editors. *Microscopic technique*. Moscow: Meditsina; 1996. EDN: LNLBTS (In Russ.)

7. Pearse AGE. *Histochemistry, theoretical and applied: theoretical and applied*. Edinburgh: Churchill Livingstone; 1968.

8. Luppa K. *Fundamentals of histochemistry*. Moscow: Mir; 1980. (In Russ.)
9. Shakhov VP, Khlusov IA, Dambaev GT, et al. *Introduction to cell culture methods, organ and tissue bioengineering*. Tomsk: STT; 2004. EDN: TVBSRX (In Russ.)
10. Korkmaz S, Goksuluk D, Zararsiz G. MVN: An R package for assessing multivariate normality. *The R Journal*. 2014;6(2):151–162. doi: 10.32614/RJ-2014-031
11. Documentation for package 'stats' version 4.4.1. The R Stats Package [Internet, cited 21.07.2024]. Available from: https://search.r-project.org/R/refmans/stats/html/00Index.html
12. brunnermunzel (version 2.0). Rdocumentation [Internet, cited 21.07.2024]. Available from: https://www.rdocumentation.org/packages/brunnermunzel/versions/2.0
13. Royston P. A remark on algorithm AS 181: The *W*-test for normality. *J Ro Stat Soc Series C Appl Stat*. 1995;44(4):547–551. doi: 10.2307/2986146
14. Moser BK, Stevens GR. Homogeneity of Variance in the Two-Sample Means Test. *Am Stat*. 1992;46(1):19–21. doi: 10.1080/00031305.1992.10475839
15. Coombs WT, Algina J, Oltman DO. Univariate and Multivariate Omnibus Hypothesis Tests Selected to Control Type I Error Rates when Population Variances are not Necessarily Equal. *Rev Educ Res*. 1996;66(2):137–179. doi: 10.3102/00346543066002137
16. Markowski CA, Markowski EP. Conditions for the Effectiveness of a Preliminary Test of Variance. *Am Stat*. 1990;44(4):322–326. doi: 10.1080/00031305.1990.10475752
17. Satterthwaite FE. An approximate distribution of estimates of variance components. *Biometrics Bulleti*n. 1946;2(6):110–114. doi: 10.2307/3002019
18. Welch BL. The Significance of the Difference Between Two Means when the Population Variances are Unequal. *Biometrika*. 1938;29(3/4):350. doi:10.2307/2332010
19. Moser BK, Stevens GR, Watts CL. The two-sample t test versus satterthwaite's approximate f test. *Commun Stat Theory Methods*. 1989;18(11):3963–3975. doi: 10.1080/03610928908830135
20. Zimmerman DW, Zumbo BD. Rank transformations and the power of the Student *t* test and Welch *t'* test for non-normal populations with unequal variances. *Can J Exp Psychol*. 1993;47(3):523–539. doi: 10.1037/h0078850
21. Munzel U, Brunner E. Nonparametric Tests in the unbalanced multivariate one-way design. *Biom J*. 2000;42(7):837–854. doi: 10.1002/1521-4036(200011)42:7<837::AID-BIMJ837>3.0.CO;2-S
22. Brunner E, Munzel U. The Nonparametric Behrens-Fisher Problem: Asymptotic Theory and a Small-Sample Approximation. *Biom J*. 2000;42(1):17–25. doi: 10.1002/(SICI)1521-4036(200001)42:1<17::AID-BIMJ17>3.0.CO;2-U
23. Karch JD. Psychologists Should Use Brunner-Munzel's Instead of Mann-Whitney's U Test as the Default Nonparametric Procedure. *Adv Methods Pract Psychol Sci*. 2021;4(2):1–14. doi: 10.1177/2515245921999602
24. Noguchi K, Konietschke F, Marmolejo-Ramos F, Pauly M. Permutation tests are robust and powerful at 0.5% and 5% significance levels. *Behav Res Methods*. 2021;53(6):2712–2724. doi: 10.3758/s13428-021-01595-5
25. Riggs BL, Melton LD. *Osteoporosis: etiology, diagnosis, treatment*. Leparskiy EA, editor. St Petersburg: BINOM; 2000. (In Russ.)
26. Ruggiero C, Bonamassa L, Pelini L, et al. Early post-surgical cognitive dysfunction is a risk factor for mortality among hip fracture hospitalized older persons. *Osteoporos Int*. 2016;28(2):667–675. doi: 10.1007/s00198-016-3784-3
27. Qi H, Jin S, Yin C, Chen L, et al. Radial extracorporeal shock wave therapy promotes osteochondral regeneration of knee joints in rabbits. *Exp Ther Med*. 2018;16(4):3478–3484. doi: 10.3892/etm.2018.6631
28. Drouzhinina TV, Khlousov IA, Karlov AV, Rostovtsev AV. Osteogenesis markers in peripheral blood as pathogenetic factors and predictors of the systemic effects of implants for osteosynthesis. *Genij Ortopedii*. 2007;(4):83–88. EDN: JHKHJR (In Russ.)
29. Tang Y, Wu X, Lei W, et al. TGF-beta1–induced migration of bone mesenchymal stem cells couples bone resorption with formation. *Nat Med*. 2009;15(7):757–765. doi: 10.1038/nm.1979
30. Li X, Yao J, Wu J, et al. Roles of PRF and IGF-1 in promoting alveolar osteoblast growth and proliferation and molecular mechanism. *Int J Clin Exp Pathol*. 2018;11(7):3294–3301.
31. Zhang Z, Zhang X, Zhao D, et al. TGF-β1 promotes the osteoinduction of human osteoblasts via the PI3K/AKT/mTOR/S6K1 signalling pathway. *Mol Med Rep*. 2019;19(5):3505–3518. doi: 10.3892/mmr.2019.10051
32. Goldberg ED, Udut VV, Khlusov IA, et al. *Patterns of structural organization of life support systems in the norm and during the development of the pathological process*. Tomsk: National Research Tomsk State University; 1996. (In Russ.) EDN: TYKLDR
33. Khlusov IA, Litvinova LS, Shupletsova VV, et al. Costimulatory Effect of Rough Calcium Phosphate Coating and Blood Mononuclear Cells on Adipose-Derived Mesenchymal Stem Cells In Vitro as a Model of In Vivo Tissue Repair. *Materials (Basel)*. 2020;13(19):4398. doi: 10.3390/ma13194398
34. Loi F, Cordova LA, Pajarinen J, et al. Inflammation, fracture and bone repair. *Bone*. 2016;86:119–130. doi: 10.1016/j.bone.2016.02.020
35. Mizuno K, Mineo K, Tachibana T, et al. The osteogenetic potential of fracture haematoma. Subperiosteal and intramuscular transplantation of the haematoma. *J Bone Joint Surg*. 1990;72(5):822–829. doi: 10.1302/0301-620x.72b5.2211764
36. Schmidt-Bleek K, Schell H, Lienau J, et al. Initial immune reaction and angiogenesis in bone healing. *J Tissue Eng Reg Med*. 2012;8(2):120–130. doi: 10.1002/term.1505
37. Schell H, Duda GN, Peters A, et al. The haematoma and its role in bone healing. *J Exp Orthop*. 2017;4(1):5. doi: 10.1186/s40634-017-0079-3
38. Sadis S, Hickey E, Weber LA. Effect of heat shock on RNA metabolism in HeLa cells. *J Cell Physio*l. 1988;135(3):377–386. doi: 10.1002/jcp.1041350304
39. Traganos F, Crissman HA, Darzynkiewicz Z. Staining with pyronin Y detects changes in conformation of RNA during mitosis and hyperthermia of CHO cells. *Exp Cell Res*. 1988;179(2):535–544. doi: 10.1016/0014-4827(88)90291-1
40. Cosgrove JW, Heikkila JJ, Brown IR. Translation of mRNA associated with monosomes and residual polysomes following disaggregation of brain polysomes by LSD and hyperthermia. *Neurochem Res*. 1982;7(4):505–518. doi: 10.1007/bf00965502

СПИСОК ЛИТЕРАТУРЫ

1. Menéndez S.T., Gallego B., Murillo D., et al. Cancer stem cells as a source of drug resistance in bone sarcomas // J Clin Med. 2021. Vol. 10, N 12. ID: 2621. doi: 10.3390/jcm10122621
2. Ringe K.I., Panzica M., von Falck C. Thermoablation of Bone Tumors // Rofo. 2016. Vol. 188, N 6. P. 539–550. doi: 10.1055/s-0042-100477
3. Kendal J.K., Singla A., Affan A., et al. Is Use of BMP-2 Associated with Tumor Growth and Osteoblastic Differentiation in Murine Models of Osteosarcoma? // Clin Orthop Relat Res. 2020. Vol. 478, N 12. P. 2921–2933. doi: 10.1097/CORR.0000000000001422
4. Pakhmurin D., Pakhmurina V., Kashin A., et al. Mechanical and Histological Characteristics of Human Tubular Bones after Hyperthermal Treatment // Symmetry. 2023. Vol. 15, N 1. ID: 156. doi: 10.3390/sym15010156
5. Пахмурин Д.О., Пахмурина В.В., Анисеня И.И., Ситников П.К. Экспериментальное изучение распределения температуры в длинных трубчатых костях при периоссальном расположении нагревателей // Сибирский онкологический журнал. 2023. Т. 22, №. 2. С. 65–75. EDN: TLRZUE doi: 10.21294/1814-4861-2023-22-2-65-75
6. Микроскопическая техника / под ред. Д.С. Саркисова, Ю.Л. Перова. Москва: Медицина, 1996. EDN: LNLBTS
7. Pearse A.G.E. Histochemistry, theoretical and applied: theoretical and applied. Edinburgh: Churchill Livingstone, 1968.
8. Луппа Х. Основы гистохимии. Москва: Мир, 1980.
9. Шахов В.П., Хлусов И.А., Дамбаев Г.Ц., и др. Введение в методы культуры клеток, биоинженерии органов и тканей. Томск: СТТ, 2004. EDN: TVBSRX
10. Korkmaz S., Goksuluk D., Zararsiz G. MVN: An R package for assessing multivariate normality // The R Journal. 2014. Vol. 6, N 2. P. 151–162. doi: 10.32614/RJ-2014-031
11. Documentation for package 'stats' version 4.4.1. The R Stats Package [интернет]. Режим доступа: https://search.r-project.org/R/refmans/stats/html/00Index.html Дата обращения: 21.07.2024.
12. brunnermunzel (version 2.0). Rdocumentation [интернет]. Режим доступа: https://www.rdocumentation.org/packages/brunnermunzel/versions/2.0 Дата обращения: 21.07.2024.
13. Royston P. A remark on algorithm AS 181: The W-test for Normality // J Ro Stat Soc Series C Appl Stat. 1995. Vol. 44, N 4. P. 547–551. doi: 10.2307/2986146
14. Moser B.K., Stevens G.R. Homogeneity of Variance in the Two-Sample Means Test // Am Stat. 1992. Vol. 46, N 1. P. 19–21. doi: 10.1080/00031305.1992.10475839
15. Coombs W.T., Algina J., Oltman D.O. Univariate and Multivariate Omnibus Hypothesis Tests Selected to Control Type I Error Rates when Population Variances are not Necessarily Equal // Rev Educ Res. 1996. Vol. 66, N 2. P. 137–179. doi: 10.3102/00346543066002137
16. Markowski C.A., Markowski E.P. Conditions for the Effectiveness of a Preliminary Test of Variance // Am Stat. 1990. Vol. 44, N 4. P. 322–326. doi: 10.1080/00031305.1990.10475752
17. Satterthwaite F.E. An approximate distribution of estimates of variance components // Biometrics Bulletin. 1946. Vol. 2, N 6. P. 110–114. doi: 10.2307/3002019
18. Welch B.L. The significance of the difference between two means when the population variances are unequal // Biometrika. 1938. Vol. 29, N 3/4. P. 350–362. doi: 10.2307/2332010
19. Moser B.K., Stevens G.R., Watts C.L. The two-sample t test versus satterthwaite›s approximate f test // Commun Stat Theory Methods. 1989. Vol. 18, N 11. P. 3963–3975. doi: 10.1080/03610928908830135
20. Zimmerman D.W., Zumbo B.D. Rank transformations and the power of the Student t test and Welch t'test for non-normal populations with unequal variances // Can J Exp Psychol. 1993. Vol. 47, N 3. P. 523–539. doi: 10.1037/h0078850
21. Munzel U., Brunner E. Nonparametric tests in the unbalanced multivariate one-way design // Biom J. 2000. Vol. 42, N 7. P. 837–854. doi: 10.1002/1521-4036(200011)42:7<837::AID-BIMJ837>3.0.CO;2-S
22. Brunner E., Munzel U. The nonparametric Behrens-Fisher Problem: Asymptotic Theory and a Small-Sample Approximation // Biom J. 2000. Vol. 42, N 1. P. 17–25. doi: 10.1002/(SICI)1521-4036(200001)42:1<17::AID-BIMJ17>3.0.CO;2-U
23. Karch J.D. Psychologists Should Use Brunner-Munzel's Instead of Mann-Whitney's U Test as the Default Nonparametric Procedure // Adv Methods Pract Psychol Sci. 2021. Vol. 4, N 2. P. 1–14. doi: 10.1177/2515245921999602
24. Noguchi K., Konietschke F., Marmolejo-Ramos F., Pauly M. Permutation tests are robust and powerful at 0.5% and 5% significance levels // Behav Res Methods. 2021. Vol. 53, N 6. P. 2712–2724. doi: 10.3758/s13428-021-01595-5
25. Риггз Б. Л., Мелтон Л. Д. Остеопороз: этиология, диагностика, лечение / под ред. Е.А. Лепарского. Санкт-Петербург: БИНОМ, 2000.
26. Ruggiero C., Bonamassa L., Pelini L., et al. Early post-surgical cognitive dysfunction is a risk factor for mortality among hip fracture hospitalized older persons // Osteoporos Int. 2017. Vol. 28, N 2. P. 667–675. doi: 10.1007/s00198-016-3784-3
27. Qi H., Jin S., Yin C., et al. Radial extracorporeal shock wave therapy promotes osteochondral regeneration of knee joints in rabbits // Exp Ther Med. 2018. Vol. 16, N 4. P. 3478–3484. doi: 10.3892/etm.2018.6631
28. Дружинина Т. В. и др. Маркеры остеогенеза в периферической крови как патогенетические факторы и предикторы системных эффектов имплантатов для остеосинтеза // Гений ортопедии. 2007. №. 4. С. 83–88. EDN: JHKHJR
29. Tang Y., Wu X., Lei W., et al. TGF-beta1–induced migration of bone mesenchymal stem cells couples bone resorption with formation // Nat Med. 2009. Vol. 15, N 7. P. 757–765. doi: 10.1038/nm.1979
30. Li X., Yao J., Wu J., et al. Roles of PRF and IGF-1 in promoting alveolar osteoblast growth and proliferation and molecular mechanism // Int J Clin Exp Pathol. 2018. Vol. 11, N 7. P. 3294–3301.
31. Zhang Z., Zhang X., Zhao D., et al. TGF-β1 promotes the osteoinduction of human osteoblasts via the PI3K/AKT/mTOR/S6K1 signalling pathway // Mol Med Rep. 2019. Vol. 19, N 5. P. 3505–3518. doi: 10.3892/mmr.2019.10051
32. Гольдберг Е.Д., Удут В.В., Хлусов И.А., и др. Закономерности структурной организации систем жизнеобеспечения в норме и при развитии патологического процесса. Томск: Национальный исследовательский Томский государственный университет, 1996. EDN: TYKLDR
33. Khlusov I.A., Litvinova L.S., Shupletsova V.V., et al. Costimulatory Effect of Rough Calcium Phosphate Coating and Blood Mononuclear Cells on Adipose-Derived Mesenchymal Stem Cells In Vitro as a Model of In Vivo Tissue Repair // Materials (Basel). 2020. Vol. 13, N 19. ID: 4398. doi: 10.3390/ma13194398

34. Loi F., Cordova L.A., Pajarinen J., et al. Inflammation, fracture and bone repair // Bone. 2016. Vol. 86. P. 119–130. doi: 10.1016/j.bone.2016.02.020
35. Mizuno K., Mineo K., Tachibana T., et al. The osteogenetic potential of fracture haematoma. Subperiosteal and intramuscular transplantation of the haematoma // J Bone Joint Surg Br. 1990. Vol. 72, N 5. P. 822–829. doi: 10.1302/0301-620X.72B5.2211764
36. Schmidt-Bleek K., Schell H., Lienau J., et al. Initial immune reaction and angiogenesis in bone healing // J Tissue Eng Regen Med. 2014. Vol. 8, N 2. P. 120–130. doi: 10.1002/term.1505
37. Schell H., Duda G.N., Peters A., et al. The haematoma and its role in bone healing // J Exp Orthop. 2017. Vol. 4, N 1. ID: 5. doi: 10.1186/s40634-017-0079-3
38. Sadis S., Hickey E., Weber L.A. Effect of heat shock on RNA metabolism in HeLa cells // J Cell Physiol. 1988. Vol. 135, N 3. P. 377–386. doi: 10.1002/jcp.1041350304
39. Traganos F., Crissman H. A., Darzynkiewicz Z. Staining with pyronin Y detects changes in conformation of RNA during mitosis and hyperthermia of CHO cells // Exp Cell Res. 1988. Vol. 179, N 2. P. 535–544. doi: 10.1016/0014-4827(88)90291-1
40. Cosgrove J.W., Heikkila J.J., Brown I.R. Translation of mRNA associated with monosomes and residual polysomes following disaggregation of brain polysomes by LSD and hyperthermia // Neurochem Res. 1982. Vol. 7, N 4. P. 505–518. doi: 10.1007/BF00965502

AUTHORS' INFO

*** Igor A. Khlusov,** MD, Dr. Sci (Medicine), Professor;
address: 2 dldg. 7 Moskovskii Trakt, 634050, Tomsk, Russia;
ORCID: 0000-0003-3465-8452;
eLibrary SPIN: 8443-8910;
e-mail: khlusov.ia@ssmu.ru

Anna V. Gorokhova;
ORCID: 0000-0001-8401-7181;
eLibrary SPIN: 3543-2303;
e-mail: a.gorokhova3062@gmail.com

Temur F. Nasibov;
ORCID: 0000-0002-8056-3967;
eLibrary SPIN: 9651-1327;
e-mail: temur.nsbv@gmail.com

Ekaterina D. Porokhova;
ORCID: 0000-0002-7317-2036;
eLibrary SPIN: 5986-3903;
e-mail: porohova_e@mail.ru

Usman A. Bariev;
ORCID: 0009-0002-7547-2558;
eLibrary SPIN: 3951-4635;
e-mail: Sorry9337@mail.ru

Vladislav E. Nosov;
ORCID: 0009-0002-2762-4836;
eLibrary SPIN: 3477-1531;
e-mail: Vladothernoises@gmail.com

Denis O. Pakhmurin, Cand. Sci (Engineering), Assistant Professor;
ORCID: 0000-0002-5191-6938;
eLibrary SPIN: 9261-5513;
e-mail: pdo@ie.tusur.ru

Ilya I. Anisenya, MD, Cand. Sci. (Medicine);
ORCID: 0000-0003-3882-4665;
eLibrary SPIN: 3003-8744;
e-mail: aii@mail.tsu.ru

Pavel K. Sitnikov, MD;
ORCID: 0000-0003-0674-2067;
eLibrary SPIN: 5945-0701;
e-mail: Sitnikov.Pavel.K@yandex.ru

ОБ АВТОРАХ

*** Хлусов Игорь Альбертович,** д-р мед. наук, профессор;
адрес: Россия, 634050, Томск, ул. Московский тракт, д. 2, стр. 7;
ORCID: 0000-0003-3465-8452;
eLibrary SPIN: 8443-8910;
e-mail: khlusov.ia@ssmu.ru

Горохова Анна Владимировна;
ORCID: 0000-0001-8401-7181;
eLibrary SPIN: 3543-2303;
e-mail: a.gorokhova3062@gmail.com

Насибов Темур Фируддин оглы;
ORCID: 0000-0002-8056-3967;
eLibrary SPIN: 9651-1327;
e-mail: temur.nsbv@gmail.com

Порохова Екатерина Даниловна;
ORCID: 0000-0002-7317-2036;
eLibrary SPIN: 5986-3903;
e-mail: porohova_e@mail.ru

Бариев Усман Адамович;
ORCID: 0009-0002-7547-2558;
eLibrary SPIN: 3951-4635;
e-mail: Sorry9337@mail.ru

Носов Владислав Евгеньевич;
ORCID: 0009-0002-2762-4836;
eLibrary SPIN: 3477-1531;
e-mail: Vladothernoises@gmail.com

Пахмурин Денис Олегович, канд. техн. наук, доцент;
ORCID: 0000-0002-5191-6938;
eLibrary SPIN: 9261-5513;
e-mail: pdo@ie.tusur.ru

Аниселя Илья Иванович, канд. мед. наук;
ORCID: 0000-0003-3882-4665;
eLibrary SPIN: 3003-8744;
e-mail: aii@mail.tsu.ru

Ситников Павел Константинович;
ORCID: 0000-0003-0674-2067;
eLibrary SPIN: 5945-0701;
e-mail: Sitnikov.Pavel.K@yandex.ru

* Corresponding author / Автор, ответственный за переписку